Colloids and Surfaces B: Biointerfaces 128 (2015) 480–488

Contents lists available at ScienceDirect

Colloids and Surfaces B: Biointerfaces

journal homepage: www.elsevier.com/locate/colsurfb

Cytotoxicity of corrosion products of degradable Fe-based stents: Relevance of pH and insoluble products

Natalia S. Fagali[a], Claudia A. Grillo[a], Susana Puntarulo[b], Mónica A. Fernández Lorenzo de Mele[a,c,*]

[a] Institute for Research in Theoretical and Applied Physical Chemistry (INIFTA), CONICET, Department of Chemistry, Faculty of Pure Sciences, UNLP, CC 16, Suc. 4, 1900, La Plata, Buenos Aires, Argentina
[b] Physical Chemistry – Institute of Biochemistry and Molecular Medicine (IBIMOL), School of Pharmacy and Biochemistry, UBA-CONICET, Buenos Aires, Argentina
[c] Faculty of Engineering, UNLP, 1900 La Plata, Buenos Aires, Argentina

ARTICLE INFO

Article history:
Received 8 October 2014
Received in revised form 18 February 2015
Accepted 25 February 2015
Available online 6 March 2015

Keywords:
Biomaterials
Iron
Degradable
Cytotoxicity
Biocompatibility

ABSTRACT

Fe-based biodegradable metallic materials (Fe-BMMs) have been proposed for cardiovascular applications and are expected to disappear *via* corrosion after an appropriate period. However, *in vivo* studies showed that Fe ions release leads to accumulation of orange and brownish insoluble products at the biomaterial/cell interface. As an additional consequence, sharp changes in pH may affect the biocompatibility of these materials. In the present work, the experimental protocols were designed with the aim of evaluating the relative importance that these factors have on biocompatibility evaluation of BMMs. Mitochondrial activity (MTT assay) and thiobarbituric acid reactive substances (TBARS) assay on mammalian cells, exposed to 1–5 mM of added Fe^{3+} salt, were assessed and compared with results linked exclusively to pH effects. Soluble Fe concentration in culture medium and intracellular Fe content were also determined. The results showed that: (i) mitochondrial activity was affected by pH changes over the entire range of concentrations of added Fe^{3+} assayed, (ii) at the highest added Fe^{3+} concentrations ($\geq$3 mM), precipitation was detected and the cells were able to incorporate the precipitate, that seems to be linked to cell damage, (iii) the extent of precipitation depends on the Fe/protein concentration ratio; and (iv) lipid peroxidation products were detected over the entire range of concentrations of added Fe^{3+}. Hence, a new approach opens in the biocompatibility evaluation of Fe-based BMMs, since the cytotoxicity would not be solely a function of released (and soluble) ions but of the insoluble degradation product amount and the pH falling at the biomaterial/cell interface. The concentration of Fe-containing products at the interface depends on diffusional conditions in a very complex way that should be carefully analyzed in the future.

1. Introduction

1.1. Degradation of Fe-based stents

In the last decades, the paradigm establishing that implants must be inert and corrosion resistant has been displaced by the advent of a new class of metallic biomaterials: biodegradable metallic materials (BMMs). BMMs have been proposed for certain specific objectives such as cardiovascular and orthopedic applications. BMMs are expected to disappear *via* corrosion after providing structural support for a certain period to complete both the regeneration and the healing process. Metals are interesting due to their mechanical properties and they are intended to manufacture bone fixation screws and plates and coronary stents [1]. Two types of metals have been proposed to produce degradable devices: magnesium (Mg)- and iron (Fe)-based alloys. Previous reports evaluated the Mg [2,3] and Fe [4–10] performance in cardiovascular devices with promising results.

As BMMs are expected to disappear *via* corrosion processes, degradation products are supposed to be present in the surrounding tissue as well as systemic tissues. Once in contact with the biological environment, these products have the potential to generate reactions, the mechanisms of which are new, perhaps unexpected, and probably unknown. Thus, it is necessary to

* Corresponding author at: Institute for Research in Theoretical and Applied Physical Chemistry (INIFTA), CONICET, Department of Chemistry, Faculty of Pure Sciences, UNLP, CC 16, Suc. 4, 1900 La Plata, Buenos Aires, Argentina. Tel.: +54 221 4257430; fax: +54 221 4254642.
E-mail address: mmele@inifta.unlp.edu.ar (M.A. Fernández Lorenzo de Mele).

http://dx.doi.org/10.1016/j.colsurfb.2015.02.047
0927-7765/

investigate the potential toxicity, and inflammatory response on surrounding tissues, based on the amount of released elements or simply physical contact between the cells and metals [1]. The rate of the ions release and the probably high local concentrations of degradation products in the biomaterial surroundings, as well as possible changes in pH, should be taken into account when biocompatibility of these devices is evaluated.

1.2. Fe degradation reactions

According to the following reactions [11], Fe corrosion is accompanied by pH changes, and consequently, these changes should be found at the biomaterial/tissue interface.

$$\text{Anodicprocess}: \quad Fe \rightarrow Fe^{2+} + 2e^- \tag{1}$$

$$\text{Cathodicprocess}: \quad 1/2O_2 + H_2O + 2e^- \rightarrow 2HO^- \tag{2}$$

The corrosion includes a complex mechanism, which involves insoluble compounds formation (reactions (3) and (4)):

The released Fe^{2+} ions react with HO^- ions producing hydrous ferrous oxides ($FeO{\cdot}nH_2O$) or ferrous hydroxides ($Fe(HO)_2$) (reaction (3)).

$$Fe^{2+} + 2HO^- \rightarrow Fe(HO)_2(s) \tag{3}$$

Since the corrosion is an interfacial process, the nearest layer to the material interface is formed by $FeO{\cdot}nH_2O$ or $Fe(HO)_2$. In the outermost layer, the dissolved O_2 produces the transformation of ferrous oxohydroxide into $Fe(HO)_3$ as in reaction (4).

$$2Fe(HO)_2(s) + H_2O + 1/2O_2 \rightarrow 2Fe(HO)_3(s) \tag{4}$$

The $Fe(HO)_3$ is normally a brownish colored and the most common corrosion product present in Fe implant/tissue interface *in vivo* [8,9], but also many Fe-complexes, hydroxopolymers and oxohydroxides are formed. The prevalence of Fe-complex type depends on pH [12]. Moreover, a high concentration of Cl^- ions was found in the vicinity of the metal surface, indicating that they play an active role in the degradation mechanisms [5]. Some metal ions are able to react with Cl^- to form $FeCl_2$ according to reaction (5).

$$Fe^{2+} + 2Cl^- \rightarrow FeCl_2 \tag{5}$$

The metal chloride formed is subsequently hydrolyzed by water, generating free acid (reaction (6)) and causing localized corrosion attacks. The Fe^{2+} and Fe^{3+} salts produce acid solutions by hydrolysis with formation of corresponding hydroxides.

$$FeCl_2 + 2H_2O \rightarrow Fe(HO)_2 + 2H^+ + Cl^- \tag{6}$$

Otherwise, the presence of carbonates in medium may conduce to other insoluble products (reaction (7)).

$$Fe^{2+} + {CO_3}^{2-} \rightarrow FeCO_{3(s)} \tag{7}$$

In the present work, the assays were designed to simulate *in vitro* the changes that would occur at the biomaterial/cells interface with the aim of predicting their cytotoxic effects during Fe-based device degradation. To understand the relative importance of the different factors that may affect biocompatibility, the effects of pH changes and Fe ions added were evaluated using MTT and TBARS assays. The intracellular Fe content was measured as well as the soluble Fe concentration in culture medium with and without serum, in order to evaluate the influence of serum on Fe solubility.

2. Materials and methods

2.1. Cell culture

Chinese hamster ovary cells (CHO-K1 line) were used. They are commonly used as *in vitro* model for cyto-genotoxicity, radiosensibility and macromolecule metabolism studies [13]. Besides, it is a useful model to evaluate *in vitro* cellular toxicity and DNA damage of metals [14–18] and nanoparticles [19,20]. The cells were originally obtained from the American Type Culture Collection (ATCC, CRL 1661, Rockville, MD, USA). CHO-K1 cells were grown as monolayers in Falcon T-25 flasks with Ham F12 culture medium (GIBCO-BRL, Los Angeles, USA) supplemented with 10% inactivated fetal calf serum (FCS) (Natocor, Carlos Paz, Córdoba, Argentina), 50 IU/mL penicillin and 50 μg/mL streptomycin sulfate (complete culture medium: CM + FCS) in a humidified incubator at 37 °C and 5% CO_2 atmosphere. Cells were counted in a Neubauer haemocytometer by the exclusion Trypan Blue (Sigma, St. Louis, MO, USA) method.

2.2. Culture medium with Fe^{3+} added

In order to determine Fe^{3+} effect, the cells were exposed to different concentrations of $FeCl_3{\cdot}6H_2O$ (Sigma–Aldrich, St. Louis, MO, USA). To obtain the maximum concentration (5 mM), the appropriated amount of salt was added to a CM + FCS, pH 8.4, and suitable dilutions were employed as required (1–4 mM). The CM + FCS medium without the addition of Fe^{3+} salt, was used as control. The concentration range was selected based on previous studies on stent dissolution rate and mass transfer processes [11,21]. At least three independent experiments were performed for each experimental condition.

2.3. Culture medium with adjusted pH

The pH of the CM + FCS medium was measured after adding Fe^{3+} salt upon the whole range of concentrations (1–5 mM) tested in the control medium. To determine the pH effect, the cells were exposed to CM + FCS with pH adjusted by using H_2SO_4 0.5 M to reach the pHs values equivalent to those obtained after Fe^{3+} salt addition. At least three independent experiments were performed for each experimental condition.

2.4. Soluble Fe in culture medium

The CM + FCS media with added Fe^{3+} salt (1–5 mM) and control medium, were filtered using Whatman No. 1 paper and colorimetric measurements were done on aliquots of filtrated media. Aliquots were incubated with the same volume of HCl 0.2 N to release Fe^{3+} ions from transferrin (the main Fe transport protein present in FCS that is usually added to CM formulation). Then, desferal solution and buffer Tris–HCl pH 7.4 were added. Samples were incubated during 15 min at room temperature and absorbance was measured at $\lambda = 430$ nm. The same procedure was applied to measure soluble Fe in other aqueous media (water, FCS and CM without FCS). At least three independent experiments were performed for each experimental condition.

2.5. Corrosion of pure Fe in culture media

In order to observe the influence of serum compounds on pure Fe corrosion, Fe-rings made from pure Fe wire (Specpure, diameter: 0.5 mm, 99.99% Fe) were immersed in CM + FCS and CM without FCS. They were cultured at room temperature and observed for 7 days.

2.6. Mitochondrial activity (methyl tetrazolium assay, MTT)

The effect or Fe^{3+} salt or pH on the mitochondrial activity of CHO-K1 cells was estimated by the MTT assay. It was carried out following the protocol previously described [22,23]. Briefly, 1.5×10^3 cells/well were seeded in a 96-multiwell dish, allowed

to attach for 24 h, and treated with different Fe^{3+} salt concentrations (1–5 mM) or media with adjusted pH (5.6–8.4), for 24 h. After these treatments, the media were changed and cells were incubated with 0.5 mg/mL MTT (3-(4,5-dimethylthiazol-2-yl)-2,5-diphenyl-tetrazolium-bromide, Sigma–Aldrich, St. Louis, MO, USA) under standard culture conditions for 3 h. Cell viability was followed by the conversion of MTT to the colored formazan product by mitochondrial dehydrogenase activity. Colored product was measured in a Microplate Reader (μQuant BioTek, USA) at λ = 540 nm after cell lyses in DMSO (100 μL/well). Mitochondrial activity was shown graphically as percent of the corresponding control values (cells growing in CM + FCS without Fe^{3+} salt or CM + FCS pH 8.4). At least three independent experiments were performed with eight repetitions each.

2.7. Thiobarbituric acid-reactive substances content (TBARS)

Lipid peroxidation products were measured according to Buege and Aust [24]. This method is based on the formation of TBARS. For this assay 4×10^6 cells/Petri dish (diameter = 100 mm) were grown at 37 °C in 5% CO_2 humid atmosphere in CM + FCS media for 24 h. This medium was then replaced by different Fe^{3+} salt-containing CM + FCS media or CM + FCS with modified pH. Next, the medium was removed and cells were washed with phosphate buffer solution (PBS) and detached with trypsin (0.25%). The cellular suspension was centrifuged and 10% Triton was added. In order to ensure the complete lysis, the samples were sonicated at low potency. Lysed cells were stored at −20 °C for the subsequent total protein measurement. An aliquot of this homogenate was incubated (80 °C, water bath for 1 h) in the presence of 0.67% TBA, 0.01% butylated hydroxytoluene (to stop the reaction) and 15% trichloroacetic acid (to precipitate proteins). After cooling, 1-butanol was added, and the mixture was shaken vigorously for 30 s. Then, the samples were centrifuged; and the absorbance was measured in butanol phase at λ = 532 nm using a Microplate Reader. The value of TBARS content was expressed as nmol MDA/mg protein and it was calculated by comparing with standards prepared from tetramethoxypropane solution. All the chemicals were from Sigma–Aldrich, St. Louis, MO, USA. At least three independent experiments were performed for each experimental condition.

2.8. Intracellular Fe content

Aliquots of each homogenate were dried at 60 °C until invariable weight and a mixture of $HClO_4/HNO_3$ 1:1 was added to disintegrate organic matter. Aliquots of these solutions were incubated with 8% thioglycolic acid, acetate buffer pH 6.0 and 4 mM bathophenanthroline [25]. All the chemicals were from Sigma–Aldrich, St. Louis, MO, USA. The absorbance at λ = 535 nm were measured using a Microplate Reader and the Fe concentration was calculated by comparing with standards prepared from Fe^{3+} in HNO_3 solutions. At least three independent experiments were performed for each experimental condition.

2.9. Determination of proteins (Bradford technique)

Aliquots of each homogenate were used for total protein measurement following Bradford method [26]. The absorbance of the Coomassie Brilliant Blue G-250–protein complex solution was measured in a Microplate Reader at λ = 595 nm. Bovine serum albumin (BSA) was used as the standard. The chemicals were from Sigma–Aldrich, St. Louis, MO, USA. At least three independent experiments were performed for each experimental condition.

2.10. TEM observations

For this assay 4×10^6 cells/Petri dish (diameter = 100 mm) were grown at 37 °C in 5% CO_2 humid atmosphere in CM + FCS media for 24 h. This medium was then replaced by different Fe^{3+} salt-containing media for 24 h. Next, the medium was removed and cells were washed with PBS and monolayers were fixed with 2% glutaraldehyde in phosphate buffer 0.2 M for 2 h at 4 °C. After fixation in 1% OsO_4, samples were embedded in epoxy resin (LX 112, Ladd) and ultrathin sections (60 nm) were obtained by Ultramicrotomy (Leica EM UC7). To enhance contrast, these sections were stained with uranyl acetate solution in alcoholic solution and lead citrate and placed on 150 mesh grids. Morphologic characteristics of the cells and the distribution of particles within the cells were examined by TEM (JEOL JEM 1200 EX II). The photographs were obtained with a Erlangshen CCD camera (Model 785 ES1000W Gatan) (Servicio Central de Microscopía Electrónica, Facultad de Ciencias Veterinarias, UNLP).

3. Results

3.1. Changes in pH in CM + FCS due to the addition of Fe^{3+} salt

When different concentrations of Fe^{3+} salt were added (1–5 mM) to the CM + FCS media, significant decrease of pH was observed. The pH values corresponding to each added Fe^{3+} concentration are shown in Fig. 1 and correspond to those obtained after Fe^{3+} salt dissolution, before the incubation with cells (0 h in the graph corresponds to initial pH at each added Fe^{3+} salt concentration). All media with added Fe^{3+} were made using CM + FCS pH 8.4. The CO_2 atmosphere, necessary to normal cell growth, acidifies the media. After 3 h, the pH of the control decreased to 7.4, optimum to cellular growth and it was maintained for 24 h (data not shown). It is worth mentioning that the selected initial pH was 8.4 because if starting pH values were below 7.5 (as in the case of Fe^{3+} addition ≥2 mM), pH values after 3 h would be usually lower than 7.4, and cells would be exposed to unfavorable conditions for longer periods than those considered by the standard protocol.

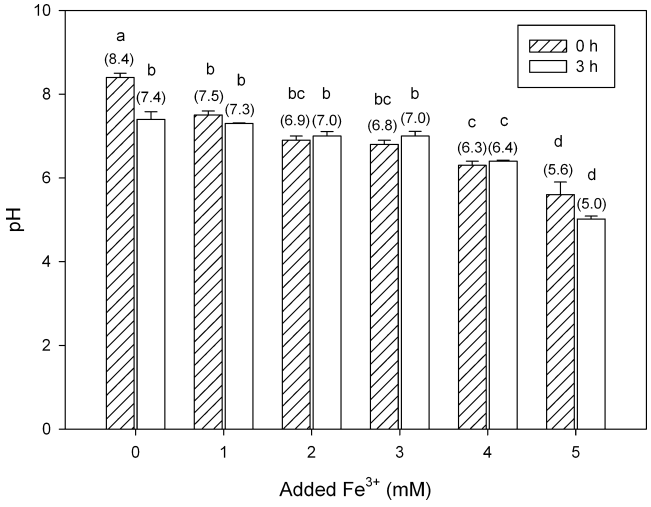

Fig. 1. pH values of CM + FCS media as a function of added Fe^{3+} salt concentration, immediately after the Fe^{3+} salt dissolution (0 h) and 3 h after this addition. Data are expressed as mean ($\bar{x}$) ± standard error of the mean (SEM). Statistical differences were analyzed using multiple comparison of Bonferroni with 99.9% of confidence. There are not statistically significant differences between data sharing identical letters in the graph.

3.2. Soluble Fe in CM and different aqueous media. Influence of presence of serum

To investigate the role of components of CM + FCS on the solubility of Fe, the concentration of soluble Fe was measured in different aqueous media. When the CM + FCS media supplemented with Fe^{3+} salts were prepared in the 3–5 mM concentrations range, the formation of precipitates was observed. All the added Fe^{3+} salt was soluble in the 1–2 mM concentration range while, surprisingly, above this range, lower solubility of Fe^{3+} salt was found (Fig. 2). In order to explain this apparently anomalous behavior, determination of soluble Fe in different aqueous media was made. Fig. 2 shows that solubilities of Fe^{3+} salt in pure FCS and in water were similar. In these media the dependence of solubility on the amount of added Fe^{3+} salt was linear. Conversely, the added salt was insoluble in CM without FCS and all the added Fe precipitated over the entire concentration range. The precipitates could be retained in the filter paper and the levels of soluble Fe were below the detectable limit. Thus, components of CM (without FCS) forms insoluble compounds with Fe^{3+} such as $Fe(HO)_3$, oxides, carbonates and/or phosphates. Notwithstanding that Fe phosphates show low solubility in water, $Fe(OH)_3$ is able to bind phosphates on its surface [27].

Moreover, solubility of Fe^{3+} in CM + FCS medium, in 1–2 mM range, was similar to that measured in water and in pure FCS. So, in this range, the Fe^{3+} salt was dissolved due to the presence of FCS in CM formulation. However, once the limit of solubility was reached, it may be expected that the soluble Fe levels remained constant, but it was not the case. When the amount of added Fe^{3+} salt reached values in the 3–5 mM range, soluble Fe levels were lower than in the 1–2 mM range. Thus, the following question arises: Do serum proteins coagulate dragging soluble Fe? To answer this question the colorimetric assay was repeated without the filtering step. The acidification step, without the filtering step of the protocol, allowed the

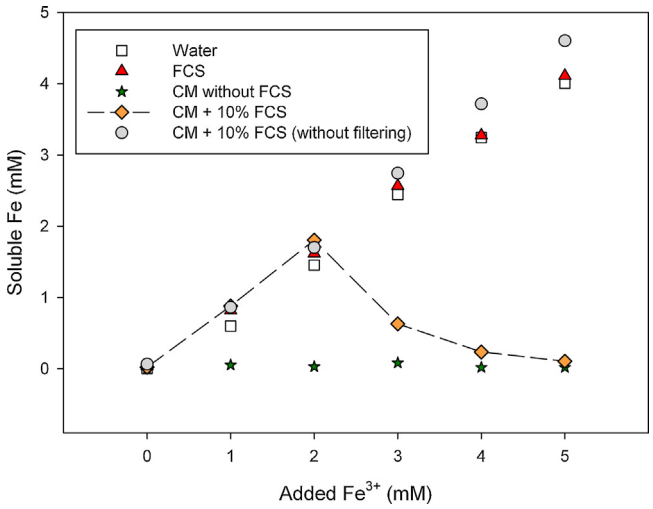

Fig. 2. Soluble Fe in different aqueous media after Fe^{3+} salt dissolution.

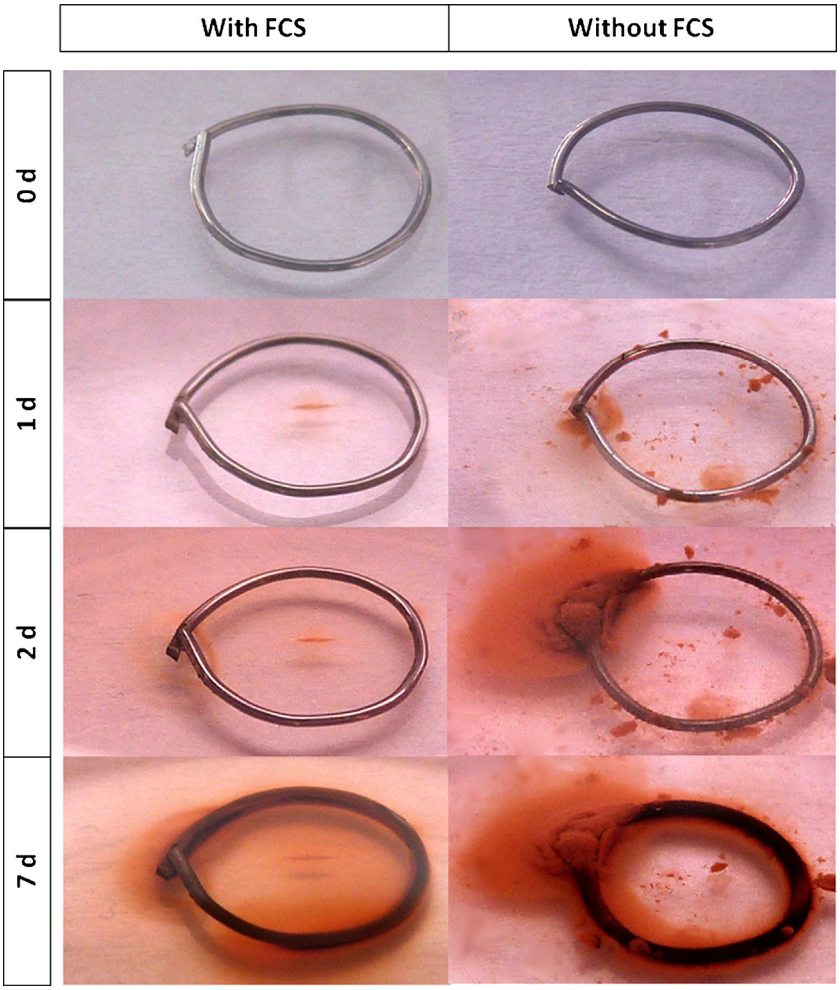

Fig. 3. Corrosion of Fe (99.99% pure) in CM with and without FCS. (For interpretation of the references to color in the text citation of this figure, the reader is referred to the web version of this article.)

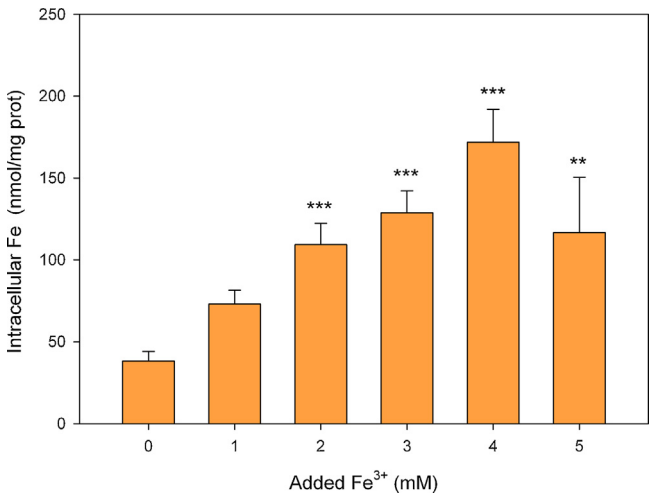

Fig. 4. Intracellular Fe content as a function of added Fe^{3+} salt concentration. Data are expressed as $\bar{x} \pm$ SEM. Statistical differences with control (0 mM) were analyzed using Bonferroni test with 99.9% (***) and 99.0% (**) of confidence.

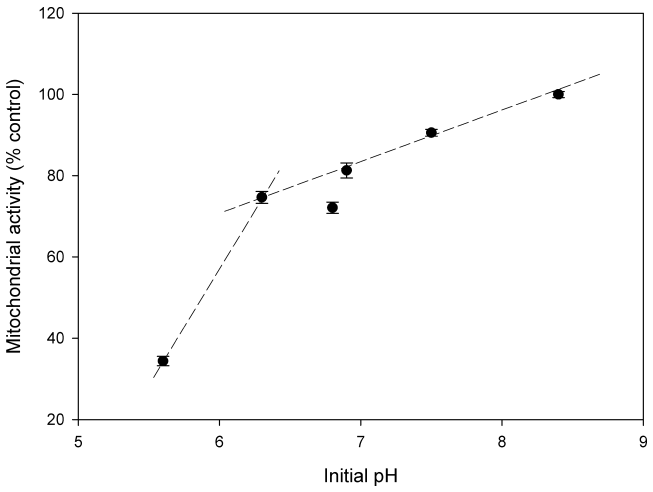

Fig. 5. Mitochondrial activity as a function of initial pH of the CM + FCS media. Data are expressed as $\bar{x} \pm$ SEM.

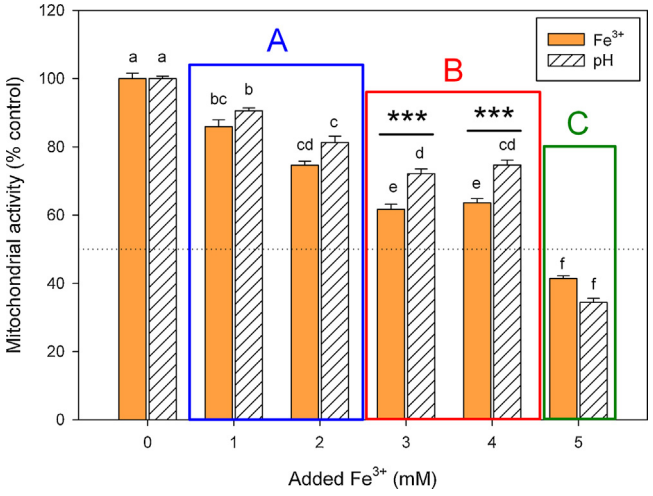

Fig. 6. Mitochondrial activity of CHO-K1 cells as a function of added Fe^{3+} salt compared to mitochondrial activity owed to pH of CM + FCS. Three areas were delimited (A, B and C) depending on the cell response to Fe^{3+} and pH. Data are expressed as $\bar{x} \pm$ SEM. Statistical differences were analyzed using multiple comparison of Bonferroni with 99.9% of confidence. There are not statistically significant differences between data sharing identical letters in the graph. Asterisks indicate significant differences between pairs.

total dissolution of Fe (including the precipitate). Fig. 2 shows that soluble Fe concentrations for 3–5 mM concentration range were similar to those obtained in water and pure FCS, confirming that serum proteins coagulate dragging soluble Fe.

3.3. Corrosion of pure Fe in the presence and in the absence of FCS

Different stages of the corrosion process of pure Fe immersed in CM with and without FCS are shown in Fig. 3. After 1 and 2 days of exposure, it can be observed a significant amount of corrosion products around the Fe-ring immersed in the CM without FCS, while only minor quantities of precipitates were formed in case of the Fe-ring immersed in the CM + FCS. After 7 days, brownish deposits are found around both rings, with higher amounts of corrosion products in the absence of FCS.

3.4. Intracellular Fe content

Data in Fig. 4 showed the intracellular Fe content in CHO-K1 cells exposed to added Fe^{3+} salt. There is not a significant difference between the assay with 1 mM of Fe^{3+} and that of the control cells. Conversely, in the 2–5 mM concentration range of added Fe^{3+} salt, the intracellular Fe was significantly higher than in control cells (2–4 mM $p < 0.001$; 5 mM $p < 0.01$). A decrease in the average value was detected for 5 mM Fe^{3+}, but significant differences with 4 mM were not found.

3.5. Mitochondrial activity in function of pH and added Fe^{3+} salt

Since the addition of different amounts of Fe^{3+} salt was accompanied by changes in pH, it was interesting to evaluate the influence of pH on cellular mitochondrial activity. For this purpose, CM + FCS media with pH values that were adjusted to attain those obtained at each concentration of added Fe^{3+} salt (see initial pHs in Fig. 1) were prepared. MTT assays with cell cultures at different pH, between 5.6 and 8.4, were performed. It could be observed (Fig. 5) that viability decreases as the pH does, with a nearly linear dependence of cell viability on pH in the 6.3–8.4 pH range. However, at pH lower than 6.3 a sharp drop of viability was detected.

Cytotoxicity evaluation was performed at different added Fe^{3+} salt concentrations (Fig. 6) in the 1 mM to 5 mM range, and it was compared with the change of mitochondrial activity associated exclusively to pH (Fig. 6). Obtained results showed that in all cases the mitochondrial activity was lower than the control without the Fe^{3+} salt (pH 8.4). The whole concentration range was divided in three regions for further analysis in Section 4.

3.6. TEM observations

TEM observations revealed that CHO-K1 cells treated with 1 mM of Fe^{3+} salt (Fig. 7) formed intracellular vesicles with dark aggregates (arrows). The architecture of the cell is similar to that of the control cell. The cells treated with 3 mM of Fe^{3+} salt showed aggregates that seem to be in vesicles and also, they are free in different sites of the cell. The ultrastructure showed drastic changes with signals of severe damage: the nucleus is difficult to identify, the cytoplasm presents vacuoles and the plasmatic membrane seems to be disintegrated. It can be observed that all aggregates are present only in the cytoplasm and it seems that they could not enter into the nucleus. The highest concentration of Fe^{3+} salt (5 mM) triggered a massive destruction of the cell: Any organelle cannot be recognized, the nucleus and cytoplasm are totally damaged. Outside the cell, it is possible to distinguish the precipitates as a background

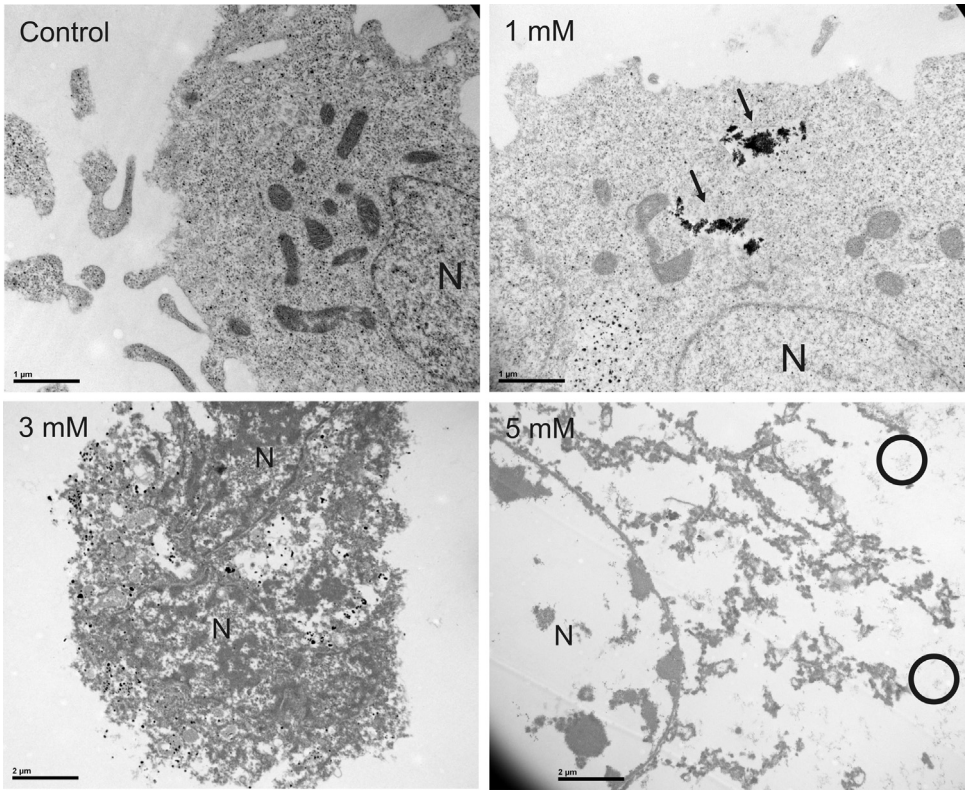

Fig. 7. TEM microphotographs from CHO-K1 cells exposed to 0, 1, 3 and 5 mM of Fe^{3+} salt for 24 h. Intracellular vesicles containing dark aggregates can be observed (arrows). N: nucleus. Fe-containing precipitates from culture medium are observed (circles) outside the cell.

(circles) while the dark aggregates cannot be seen between the disintegrated parts of the cytoplasm.

3.7. Lipid peroxidation products as a function of pH and added Fe^{3+} salt

TBARS content in CHO-K1 cells exposed to different pH (8.4–5.6 range) or different Fe^{3+} salt concentrations (1–5 mM) is shown in Fig. 8. It could be observed that TBARS production was pH independent. However, TBARS production in presence of added Fe^{3+} salt was significantly higher over the entire concentration range than that observed when using control cells.

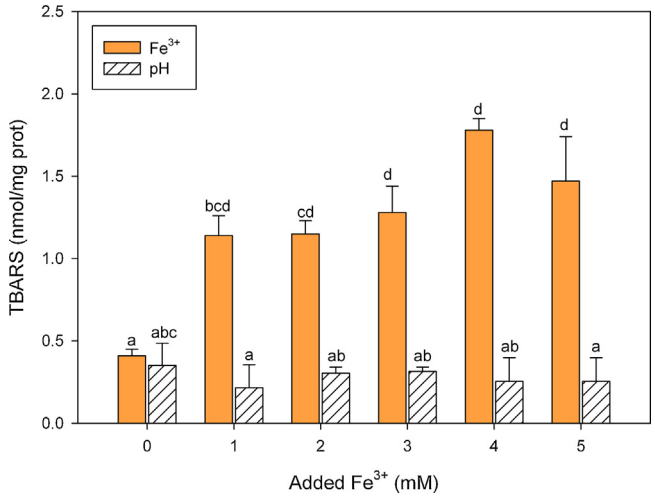

Fig. 8. TBARS production as a function of added Fe^{3+} salt compared to TBARS production owed to pH of the CM + FCS media. Data are expressed as $\bar{x} \pm$ SEM. Statistical differences were analyzed using multiple comparison of Bonferroni with 99.9% of confidence. There are not statistically significant differences between data sharing identical letters in the graphs.

4. Discussion

4.1. Metal ions release, diffusion and precipitation: the problem of studying the interface.

The analysis of Fe based-stent degradation and its consequences in biological environment is a complex problem. It should be considered that *in vivo*, close to the metal/tissue interface, ions concentration gradients are formed. In a previous paper [28] the diffusion of ions in a biological medium was simulated through a very complex relationship derived from the Fick's 2nd law equation (see supplementary information). Accordingly, when we analyze the effect of Fe ion concentration on cell viability *in vivo* we should have in mind that concentration is a function of the distance from the stent and the exposure time. Hence, if we consider a particular concentration it may have resulted under different conditions, for example: after a shorter exposure time in a place closer to the metal source or after longer exposure time and further from the implant. Moreover, the analysis of problem is even more complex if we consider that the gradients are also influenced both by the presence of biological molecules and by the solubility of the complexes that may be formed.

The amount of Fe released from implanted coronary or femoral stents is related with their weights (≈41–750 mg). If we assume 0.5 mL of biological fluid, as a rough estimation of the volume of biological medium in contact with the stent, concentrations between 4.0 and 73.0 mM could be reached every day due to release of Fe at the interface, during a degradation period of 1 year. In fact, the reported corrosion rates of Fe stent *in vivo* are lower than these

estimations but, to reach the desirable 1 year degradation period, the interface under diffusion restrictions, would be in contact with higher concentration values (as those we mentioned) as well as with the corresponding pH changes. The released metal can be found as precipitated or soluble form since that pure Fe is corrodible in fluids with high levels of O_2 (see Eqs. (1)–(7) in Section 1).

In the specific case of Fe-based alloys the analysis of the effect of Fe ions should be made considering relationships between the release rate of the alloy components and Fe, which generally do not fit with the relationships between the percent of elements of the alloy composition. Importantly, the effect of ions as single elements may be different from that of these ions in the mixture; additive or synergistic effects may be found [29,30].

4.2. Role of proteins in Fe solubility

Pierson et al. [31] reported that Fe wires in contact with flowing blood are minimally corroded while in case of those metals placed in the arterial wall degradation products were accumulated and that might challenge the long-term integrity of the artery. Consequently, degradation rate *in vivo* is strongly dependent on the environmental conditions.

Our results revealed that serum compounds, mainly proteins, are closely involved in the solubility/degradation process (Figs. 2 and 3). It has been reported that the Fe surface exposed to bloodstream is passivated by adsorption of serum proteins [32], avoiding the initial degradation products accumulation. Moreover, when the corrosion process starts, the serum compounds help to solubilize released Fe ions bounding them mainly to transferrin, an abundant, high-affinity iron-binding protein. Very small amounts of Fe may be loosely associated with albumin or small molecules [33]. This *in vivo* situation is similar to ours *in vitro* results (pure Fe incubated with CM+ FCS medium, Fig. 3). Moreover, Fe exposed to CM without FCS showed voluminous precipitates that resemble those found *in vivo* within the arterial wall [8,9,31]. Thus, the important role of proteins in the corrosion process and in the generation of insoluble products should be taken into account.

4.3. Influence of Fe concentration on cell viability

It is known the relevant role of mitochondria in cell survival. To analyze if cell viability was affected by the release of Fe-products in the biological media, mitochondrial activity was evaluated (MTT assay) (Fig. 6) after the addition of different concentrations of Fe^{3+} salt to the media. A non-linear dose-dependence response with the concentration of added Fe^{3+} salt was observed. In order to facilitate the analysis of the results, three zones (A, B and C) were delimited considering cellular response to Fe^{3+} and pH treatments (Fig. 6). The biological effects in these zones were analyzed as shown in the following sections.

4.3.1. Zone A. Low added Fe^{3+} salt concentrations range (1–2 mM)

In this concentration range, detrimental effect of Fe *per se* on mitochondrial activity was not observed; in fact, the decrease in the activity can only be attributed to the pH falling. For 2 mM, all the added Fe^{3+} salt was soluble and, the intracellular Fe amount was significantly higher than in the control cells. TEM observations (Fig. 7) confirmed that low concentrations of soluble Fe^{3+} would not be detrimental to the cells.

4.3.2. Zone B. Intermediate added Fe^{3+} salt concentrations range (3–4 mM)

The deleterious effect of added Fe^{3+} in this zone was higher than the effect owed to pH as single factor. In this concentration range, the formation of precipitates started and the amount of soluble Fe was lesser than in the zone A. Although soluble Fe diminished, intracellular Fe increased in this concentration range and TEM observations confirmed that the cells incorporated precipitates (Fig. 7). The cells exposed to 3 mM of Fe^{3+} salt showed severe signals of damage. Thus, the insoluble products could enter into the cells, as nanoparticles do, through endocytosis mechanisms. It is known that, cells are able to internalize small particles from degradable and nondegradable materials, and once within the cytoplasm they may coalesce and form larger aggregates [34–36].

Thus, in this concentration range the effects of precipitates accumulation and pH falling are more relevant factors than the effect of soluble ions.

4.3.3. Zone C. High added Fe^{3+} salt concentration (5 mM)

In this zone, an important decrease on mitochondrial activity was measured. However, no significant differences between pH and added Fe^{3+} effect were found. So, an extremely low pH (pH 5.6) is very harmful to the cells and it is independent of the Fe^{3+} presence. Soluble Fe was almost undetectable since it was dragged with protein-containing precipitates, as it was mentioned above. The intracellular Fe content was significantly higher than in the control cells ($p < 0.01$). Thus, the decrease of mitochondrial activity appears to be related to the intracellular Fe content but not to the amount of soluble Fe in the medium.

Schinhammer et al. [5] found an important relationship between pH and compatibility of biodegradable Fe-based alloys. The authors evaluated the cytocompatibility of Fe^{2+} and Fe^{3+} salts and alloys with human umbilical vein endothelial cells (HUVEC) and a lower tolerance to Fe^{3+} than to Fe^{2+} was observed, ascribing this effect to the lower pH found in Fe^{3+} solutions. They also reported that acidity of the medium was required to avoid precipitation, and red-brownish degradation products were found around the alloy in agreement with data shown in Fig. 3.

When present results were analyzed the following question arised: Is it possible that the intracellular Fe rise when the soluble Fe in the medium diminished (Zones B and C)? This apparent contradiction can be explained taking into account a new player: the precipitate. Pivokonsky et al. [12] studied the precipitation of proteins with $Fe_2(SO_4)_3$ showing that precipitation is strongly dependent on pH. The highest amount of precipitate was obtained in the 4–6 pH range, due to electrostatic neutralization between negative charges in proteins surface and hydrolysis products of Fe^{3+} positively charged. This mechanism would also explain the situation observed at 5 mM of added Fe^{3+}, where the soluble Fe amount was the lowest. At pH > 6 (3–4 mM of added Fe^{3+}), the high ratio Fe/proteins favored the adsorption of soluble Fe-protein complexes on Fe-oxohydroxides, diminishing the amount of soluble Fe. Conversely, when the ratio Fe/protein is low (1–2 mM of added Fe^{3+}), soluble Fe-complexes are formed and the steric stabilization hampered the precipitation. This reasoning would justify the trend observed in the plot corresponding to CM + 10% FCS (Fig. 2).

4.4. Influence of Fe concentration and pH on lipid peroxidation

In the entire range of concentrations added Fe^{3+} salt (1–5 mM), significantly higher TBARS production than in the control cells was detected. However, there were not significant differences among cells exposed to different pHs and control cells, therefore the medium acidification would not produce lipid peroxidation in the analyzed pH range. The average values of TBARS content did not show significant differences between the cells exposed to different added Fe^{3+} concentrations. However, despite the high variability in TBARS and intracellular Fe results, TBARS production (Fig. 8) followed the same profile that intracellular Fe content (Fig. 4) that is different from the soluble Fe trend. Thus, it could be assumed that higher intracellular Fe is related to greater oxidative damage

to lipids, although more specific assays are required to assess oxidative damage of Fe degradation products.

5. Conclusions

To achieve total degradation of a biodegradable Fe-based stent in 1 year period, a high corrosion rate is necessary. This implicates an important accumulation of particles of fragmented material and soluble and insoluble degradation products, apart from the pH falling in adjacent tissues to the implant.

- Results reported here demonstrated that mitochondrial activity was affected by pH changes at the entire Fe^{3+} concentrations range assayed.
- At the highest added Fe^{3+} concentrations ($\geq$3 mM), precipitation was detected and the cells were able to incorporate the precipitate. This factor may be linked to cell damage.
- The extent of precipitation strongly depends on the Fe/protein concentration ratio: high Fe/protein ratio favors precipitation while low Fe/protein ratio promotes Fe^{3+} solubilization.
- Lipid peroxidation products were detected over the entire range of concentrations of added Fe^{3+}. The TBARS production was pH-independent and seems to be related to intracellular Fe content.

The concentration of soluble and insoluble corrosion products is dependent on the exposure time and distance from the degradable metal following a very complex relationship. Considering that *in vivo* there are concentration gradients (Fe^{3+}, degradation products, pH, *etc.*), cytotoxicity evaluation should be focused on the interface biomaterial/tissue rather than on the systemic level of soluble Fe. As these processes are difficult to evaluate *in vivo, in vitro* studies, such as that presented in this work, are useful tools to rationalize these problems. Thus, a new approach is proposed here to investigate the biocompatibility of Fe-based BMMs, since the cytotoxicity is not exclusively focused in soluble released ions but on the processes that involve pH changes and insoluble product formation.

Acknowledgments

The authors would want to acknowledge to Dr. Angel Catalá for his helpful assistance and collaboration. This study was supported by grants from the University of La Plata (UNLP, 11/I163), University of Buenos Aires (UBA, UBACyT 555), ANPCyT (PICT 2012-1795 BID, PICT 00845, PPL 2011 0003) and CONICET (PIP 00697)

Appendix A. Supplementary data

Supplementary data associated with this article can be found, in the online version, at http://dx.doi.org/10.1016/j.colsurfb.2015.02.047.

References

[1] A. Purnama, H. Hermawan, J. Couet, D. Mantovani, Assessing the biocompatibility of degradable metallic materials: state-of-the-art and focus on the potential of genetic regulation, Acta Biomater. 6 (2010) 1800–1807, http://dx.doi.org/10.1016/j.actbio.2010.02.027.

[2] P. Zartner, R. Cesnjevar, H. Singer, M. Weyand, First successful implantation of a biodegradable metal stent into the left pulmonary artery of a preterm baby, Catheter. Cardiovasc. Interv. 66 (2005) 590–594, http://dx.doi.org/10.1002/ccd.20520.

[3] D. Schranz, P. Zartner, I. Michel-Behnke, H. Akintürk, Bioabsorbable metal stents for percutaneous treatment of critical recoarctation of the aorta in a newborn, Catheter. Cardiovasc. Interv. 67 (2006) 671–673, http://dx.doi.org/10.1002/ccd.20756.

[4] T. Huang, J. Cheng, Y.F. Zheng, In vitro degradation and biocompatibility of Fe–Pd and Fe–Pt composites fabricated by spark plasma sintering, Mater. Sci. Eng. C: Mater. Biol. Appl. 35 (2014) 43–53, http://dx.doi.org/10.1016/j.msec.2013.10.023.

[5] M. Schinhammer, P. Steiger, F. Moszner, J.F. Löffler, P.J. Uggowitzer, Degradation performance of biodegradable Fe–Mn–C(–Pd) alloys, Mater. Sci. Eng. C: Mater. Biol. Appl. 33 (2013) 1882–1893, http://dx.doi.org/10.1016/j.msec.2012.10.013.

[6] M. Schinhammer, I. Gerber, A.C. Hänzi, P.J. Uggowitzer, On the cytocompatibility of biodegradable Fe-based alloys, Mater. Sci. Eng. C 33 (2013) 782–789, http://dx.doi.org/10.1016/j.msec.2012.11.002.

[7] M. Peuster, P. Wohlsein, M. Brügmann, M. Ehlerding, K. Seidler, C. Fink, et al., A novel approach to temporary stenting: degradable cardiovascular stents produced from corrodible metal-results 6–18 months after implantation into New Zealand white rabbits, Heart 86 (2001) 563–569, http://dx.doi.org/10.1136/heart.86.5.563.

[8] M. Peuster, C. Hesse, T. Schloo, C. Fink, P. Beerbaum, C. von Schnakenburg, Long-term biocompatibility of a corrodible peripheral iron stent in the porcine descending aorta, Biomaterials 27 (2006) 4955–4962, http://dx.doi.org/10.1016/j.biomaterials.2006.05.029.

[9] R. Waksman, R. Pakala, R. Baffour, R. Seabron, D. Hellinga, F.O. Tio, Short-term effects of biocorrodible iron stents in porcine coronary arteries, J. Interv. Cardiol. 21 (2008) 15–20, http://dx.doi.org/10.1111/j.1540-8183.2007.00319.x.

[10] M. Zhang, N. Cresswell, F. Tavora, E. Mont, Z. Zhao, A. Burke, In-stent restenosis is associated with neointimal angiogenesis and macrophage infiltrates, Pathology (2014) 1–5.

[11] M. Moravej, A. Purnama, M. Fiset, J. Couet, D. Mantovani, Electroformed pure iron as a new biomaterial for degradable stents: in vitro degradation and preliminary cell viability studies, Acta Biomater. 6 (2010) 1843–1851, http://dx.doi.org/10.1016/j.actbio.2010.01.008.

[12] M. Pivokonsky, J. Safarikova, P. Bubakova, L. Pivokonska, Coagulation of peptides and proteins produced by *Microcystis aeruginosa*: interaction mechanisms and the effect of Fe-peptide/protein complexes formation, Water Res. 46 (2012) 5583–5590, http://dx.doi.org/10.1016/j.watres.2012.07.040.

[13] X. Jiang, T. Miclăuș, L. Wang, R. Foldbjerg, D.S. Sutherland, H. Autrup, et al., Fast intracellular dissolution and persistent cellular uptake of silver nanoparticles in CHO-K1 cells: implication for cytotoxicity, Nanotoxicology (2014), http://dx.doi.org/10.3109/17435390.2014.907457.

[14] A.J. García-Fernández, A.E. Bayoumi, Y. Pérez-Pertejo, M. Motas, R.M. Reguera, C. Ordóñez, et al., Alterations of the glutathione-redox balance induced by metals in CHO-K1 cells, Comp. Biochem. Physiol. C: Toxicol. Pharmacol. 132 (2002) 365–373, http://www.ncbi.nlm.nih.gov/pubmed/12161170

[15] C.M. Thompson, Y. Fedorov, D.D. Brown, M. Suh, D.M. Proctor, L. Kuriakose, et al., Assessment of Cr(VI)-induced cytotoxicity and genotoxicity using high content analysis, PLoS ONE 7 (2012) e42720, http://dx.doi.org/10.1371/journal.pone.0042720.

[16] S. Soodvilai, J. Nantavishit, C. Muanprasat, V. Chatsudthipong, Renal organic cation transporters mediated cadmium-induced nephrotoxicity, Toxicol. Lett. 204 (2011) 38–42, http://dx.doi.org/10.1016/j.toxlet.2011.04.005.

[17] J.L. Yang, J.I. Chao, J.G. Lin, Reactive oxygen species may participate in the mutagenicity and mutational spectrum of cadmium in Chinese hamster ovary-K1 cells, Chem. Res. Toxicol. 9 (1996) 1360–1367, http://dx.doi.org/10.1021/tx960122y.

[18] C.A. Grillo, M.A. Reigosa, M.A.F.L. de Mele, Does over-exposure to copper ions released from metallic copper induce cytotoxic and genotoxic effects on mammalian cells? Contraception 81 (2010) 343–349, http://dx.doi.org/10.1016/j.contraception.2009.12.003.

[19] X. Jiang, R. Foldbjerg, T. Miclaus, L. Wang, R. Singh, Y. Hayashi, et al., Multi-platform genotoxicity analysis of silver nanoparticles in the model cell line CHO-K1, Toxicol. Lett. 222 (2013) 55–63, http://dx.doi.org/10.1016/j.toxlet.2013.07.011.

[20] D.-W. Han, Y.I. Woo, M.H. Lee, J.H. Lee, J. Lee, J.-C. Park, In-vivo and in-vitro biocompatibility evaluations of silver nanoparticles with antimicrobial activity, J. Nanosci. Nanotechnol. 12 (2012) 5205–5209, http://www.ncbi.nlm.nih.gov/pubmed/22966546

[21] G.J. Anderson, D.M. Frazer, G.D. McLaren, Iron absorption and metabolism, Curr. Opin. Gastroenterol. 25 (2009) 129–135, http://dx.doi.org/10.1097/MOG.0b013e32831ef1f7.

[22] T. Mosmann, Rapid colorimetric assay for cellular growth and survival: application to proliferation and cytotoxicity assays, J. Immunol. Methods 65 (1983) 55–63, http://dx.doi.org/10.1016/0022-1759(83)90303-4.

[23] P.R. Twentyman, M. Luscombe, A study of some variables in a tetrazolium dye (MTT) based assay for cell growth and chemosensitivity, Br. J. Cancer 56 (1987) 279–285, http://dx.doi.org/10.1038/bjc.1987.190.

[24] J.A. Buege, S.D. Aust, Microsomal lipid peroxidation, Methods Enzymol. 52 (1978) 302–310, http://www.ncbi.nlm.nih.gov/pubmed/672633

[25] P.E. Brumby, V. Massey, Determination of nonheme iron, total iron, and copper, Methods Enzymol. 10 (1967) 463–474, http://dx.doi.org/10.1016/0076-6879(67)10078-5.

[26] M.M. Bradford, A rapid and sensitive method for the quantitation of microgram quantities of protein utilizing the principle of protein–dye binding, Anal. Biochem. 72 (1976) 248–254, http://dx.doi.org/10.1016/0003-2697(76)90527-3.

[27] T. Kraus, F. Moszner, S. Fischerauer, M. Fiedler, E. Martinelli, J. Eichler, et al., Biodegradable Fe-based alloys for use in osteosynthesis: outcome of an in vivo study after 52 weeks, Acta Biomater. 10 (2014) 3346–3353, http://dx.doi.org/10.1016/j.actbio.2014.04.007.

[28] M.D. Pereda, M. Reigosa, M. Fernández Lorenzo de Mele, Relationship between radial diffusion of copper ions released from a metal disk and cytotoxic

effects. Comparison with results obtained using extracts, Bioelectrochemistry 72 (2008) 94–101, http://dx.doi.org/10.1016/j.bioelechem.2007.11.008.
[29] C.A. Grillo, F. Alvarez, M.A.F.L. de Mele, Cellular response to rare earth mixtures (La and Gd) as components of degradable Mg alloys for medical applications, Colloids Surf. B: Biointerfaces. 117 (2014) 312–321, http://dx.doi.org/10.1016/j.colsurfb.2014.02.030.
[30] C.A. Grillo, M.L. Morales, M.V. Mirífico, M.A. Fernández Lorenzo de Mele, Synergistic cytotoxic effects of ions released by zinc-aluminum bronze and the metallic salts on osteoblastic cells, J. Biomed. Mater. Res. A 101 (2013) 2129–2140, http://dx.doi.org/10.1002/jbm.a.34503.
[31] D. Pierson, J. Edick, A. Tauscher, E. Pokorney, P. Bowen, J. Gelbaugh, et al., A simplified in vivo approach for evaluating the bioabsorbable behavior of candidate stent materials, J. Biomed. Mater. Res. B: Appl. Biomater. 100 (2012) 58–67, http://dx.doi.org/10.1002/jbm.b.31922.
[32] S. Zhu, N. Huang, L. Xu, Y. Zhang, H. Liu, Y. Lei, et al., Biocompatibility of Fe–O films synthesized by plasma immersion ion implantation and deposition, Surf. Coat. Technol. 203 (2009) 1523–1529, http://dx.doi.org/10.1016/j.surfcoat.2008.11.033.
[33] N.C. Andrews, P.J. Schmidt, Iron homeostasis, Annu. Rev. Physiol. 69 (2007) 69–85, http://dx.doi.org/10.1146/annurev.physiol.69.031905.164337.
[34] A.L. Di Virgilio, M. Reigosa, M.F.L. de Mele, Response of UMR 106 cells exposed to titanium oxide and aluminum oxide nanoparticles, J. Biomed. Mater. Res. A. 92 (2010) 80–86, http://dx.doi.org/10.1002/jbm.a.32339.
[35] A.L. Di Virgilio, M. Reigosa, P.M. Arnal, M. Fernández Lorenzo de Mele, Comparative study of the cytotoxic and genotoxic effects of titanium oxide and aluminium oxide nanoparticles in Chinese hamster ovary (CHO-K1) cells, J. Hazard. Mater. 177 (2010) 711–718, http://dx.doi.org/10.1016/j.jhazmat.2009.12.089.
[36] A.L. Di Virgilio, M. Reigosa, M.F.L. de Mele, Biocompatibility of magnesium particles evaluated by in vitro cytotoxicity and genotoxicity assays, J. Biomed. Mater. Res. B: Appl. Biomater. 99 (2011) 111–119, http://dx.doi.org/10.1002/jbm.b.31877.